the plant journal

SEB SOCIETY FOR EXPERIMENTAL BIOLOGY

The Plant Journal (2024) doi: 10.1111/tpj.16608

Identification and evolution of a diterpenoid phytoalexin oryzalactone biosynthetic gene in the genus *Oryza*

Keisuke Kariya[1], Haruka Mori[2], Makoto Ueno[3], Takanori Yoshikawa[4], Masayoshi Teraishi[5], Yukinori Yabuta[2], Kotomi Ueno[2] and Atsushi Ishihara[2,*]

[1]*The United Graduate School of Agricultural Sciences, Tottori University, 4-110 Koyama Minami, Tottori 680-8553, Japan,*
[2]*Faculty of Agriculture, Tottori University, 4-110 Koyama Minami, Tottori 680-8553, Japan,*
[3]*Faculty of Life and Environmental Sciences, Shimane University, Nishikawatsu 1060, Matsue 690-8504, Japan,*
[4]*National Institute of Genetics, 1111 Yata, Mishima, Shizuoka 411-8540, Japan, and*
[5]*Graduate School of Agriculture, Kyoto University, Kitashirakawa Oiwake-Cho, Kyoto 606-8502, Japan*

Received 24 August 2023; revised 11 November 2023; accepted 14 December 2023.
*For correspondence (e-mail aishihara@tottori-u.ac.jp).

SUMMARY

The natural variation of plant-specialized metabolites represents the evolutionary adaptation of plants to their environments. However, the molecular mechanisms that account for the diversification of the metabolic pathways have not been fully clarified. Rice plants resist attacks from pathogens by accumulating diterpenoid phytoalexins. It has been confirmed that the composition of rice phytoalexins exhibits numerous natural variations. Major rice phytoalexins (momilactones and phytocassanes) are accumulated in most cultivars, although oryzalactone is a cultivar-specific compound. Here, we attempted to reveal the evolutionary trajectory of the diversification of phytoalexins by analyzing the oryzalactone biosynthetic gene in *Oryza* species. The candidate gene, *KSLX-OL*, which accounts for oryzalactone biosynthesis, was found around the single-nucleotide polymorphisms specific to the oryzalactone-accumulating cultivars in the long arm of chromosome 11. The metabolite analyses in *Nicotiana benthamiana* and rice plants overexpressing *KSLX-OL* indicated that *KSLX-OL* is responsible for the oryzalactone biosynthesis. *KSLX-OL* is an allele of *KSL8* that is involved in the biosynthesis of another diterpenoid phytoalexin, oryzalexin S and is specifically distributed in the AA genome species. *KSLX-NOL* and *KSLX-bar*, which encode similar enzymes but are not involved in oryzalactone biosynthesis, were also found in AA genome species. The phylogenetic analyses of *KSLX*s, *KSL8*s, and related pseudogenes (*KSL9*s) indicated that *KSLX-OL* was generated from a common ancestor with *KSL8* and *KSL9* via gene duplication, functional differentiation, and gene fusion. The wide distributions of *KSLX-OL* and *KSL8* in AA genome species demonstrate their long-term coexistence beyond species differentiation, suggesting a balancing selection between the genes.

Keywords: rice (*Oryza sativa* L.), phytoalexin, evolution, balancing selection, diterpenoid.

INTRODUCTION

Every plant species accumulates diverse and characteristic specialized metabolites, with the estimated number of specialized metabolites produced by plants being 200 000–1 million (Wang et al., 2019). Some of these metabolites are universally distributed within the plant kingdom, whereas others are species-specific. As plants cannot select the environment in which they grow, their accumulation of various specialized metabolites is considered a crucial survival strategy for adapting to their habitat. The specialized metabolites that accumulate in plants are classified as terpenoids, flavonoids, benzenoids, phenylpropanoids, nitrogen-containing compounds, etc., based on their chemical structures (Wang et al., 2019). These metabolites exhibit diverse bioactivities, including antimicrobial activities, attractant or repellent activities on other organisms, and promoting or inhibitory activities for the growth and development of plants (Jain et al., 2018).

The compositions of specialized metabolites among the cultivars or strains within a species exhibit variations. Their compositions can differ greatly in the subgroups of a species with diverse habitats and distinct evolutionary histories. Kliebenstein, Kroymann, et al. (2001) quantitatively analyzed 34 glucosinolates in the leaves and seeds of 39 ecotypes of *Arabidopsis thaliana* (L.) Heynh. and demonstrated the existence of natural variation in the composition of glucosinolates. The differences in the amount of accumulated glucosinolates among the ecotypes ranged

from 2.5- to 1220-fold (except when the values were below the limit of detection).

Plants accumulate low-molecular-weight antimicrobial compounds, phytoalexins, to respond to pathogens. It has been confirmed that various plants accumulate phytoalexins (Ahuja et al., 2012). More than 20 compounds, mostly diterpenoids, have been reported as phytoalexins in rice (*Oryza sativa* L.) (Kariya et al., 2020, 2023; Valletta et al., 2023). The production of phytoalexins is induced by a pathogen attack, ultraviolet (UV) light irradiation, and treatment with phytohormones, such as jasmonic acid (Akagi et al., 2014).

World Rice Core Collection (WRC) is a suitable material for investigating the natural variation of various rice traits. WRC comprises 69 accessions, retaining 90% of the restriction fragment length polymorphism alleles detected in ~300 accessions that were selected based on the passport data from the entire rice collection (~30 000 accessions) maintained at the National Agriculture and Food Research Organization (NARO) in Japan (Kojima et al., 2005). The intraspecific diversity of rice phytoalexins has been revealed by investigation of WRC (Kariya et al., 2019, 2020, 2023; Murata et al., 2019). For instance, most cultivars accumulate diterpenoid phytoalexins (momilactone A and phytocassane A) to respond to UV light irradiation, although only three of the 69 cultivars in WRC accumulated oryzalactone (Kariya et al., 2020). In jasmonic acid-treated leaves, some of the cultivars accumulated sakuranetin, whereas the others accumulated naringenin, which is the immediate precursor of sakuranetin (Murata et al., 2019). As natural variation reflects the process by which an organism adapts to its habitat, the analysis thereof may offer insight into the adaptive evolutionary process. However, the biochemical and biological bases that result in the diversification of chemotypes in rice have not been sufficiently addressed.

The presence of multiple genes encoding for diterpene cyclases enables rice plants to biosynthesize diverse diterpenoids with distinct carbon skeletons. Tricyclic diterpenes are biosynthesized by copalyl pyrophosphate (CPP) synthase (CPS) and kaurene synthase-like (KSL) from geranylgeranyl pyrophosphate (GGPP). The rice genome contains four CPSs and 11 KSLs, and their functions have been analyzed. CPS2 and CPS4 contribute to the production of phytoalexins by catalyzing the conversions of GGPP into *ent*-CPP and *syn*-CPP, respectively; both products exhibit different steric configurations (Otomo et al., 2004). Among the *KSLs*, *KSL3* and *KSL9* are pseudogenes (Sakamoto et al., 2004; Xu, Wilderman, Morrone, et al., 2007), and the products of the remaining nine *KSLs* differ (Toyomasu et al., 2020). Four of these genes, *KSL4*, *KSL7*, *KSL8*, and *KSL10*, are involved in the biosynthesis of phytoalexins. *KSL8* and *KSL10* contain two alleles, which encode the enzymes that catalyze distinct reactions (Toyomasu et al., 2016).

Rice belongs to the genus *Oryza* belonging to the tribe Oryzeae of the subfamily Ehrhartoideae of the Poaceae family. The genus *Oryza* includes 23 species, which are classified into 10 genome types, six diploid types (AA, BB, CC, EE, FF, and GG), and four tetraploid types (BBCC, CCDD, HHJJ, and KKLL) (Aggarwal et al., 1997; Ammiraju et al., 2010). The BB genome type (*O. punctata*) is most closely related to the AA genome type containing two cultivated species (*O. sativa* and *O. glaberrima*), whereas the FF genome type (*O. brachyantha*) diverged from other genome types at the basal part of the phylogenetic tree of the genus (Stein et al., 2018). The biosynthesis of rice phytoalexins has been studied from the evolutionary perspective by analyzing phytoalexin accumulation and their biosynthetic genes in the related species. Miyamoto et al. (2016) proposed the evolutionary trajectory of the momilactone and phytocassane biosynthetic gene clusters (BGCs) in the genus *Oryza* species. The momilactone BGC is believed to have been acquired by the common ancestors of the AA and BB genome species. Momilactone BGC has been found in the genus *Oryza* as well as bryophytes *Calohypnum plumiforme* and barnyardgrass *Echinochloa crus-galli*, and the BGCs may have emerged from convergent evolution and horizontal gene transfer, respectively (Mao et al., 2020; Wu et al., 2022). All the genes in the BGC of *ent*-10-oxodepressin (5,10-diketocasbene) originated from the genus *Oryza*, and the cluster is at least partially formed in the wild rice ancestor, *O. rufipogon* (Zhan et al., 2020). In contrast, the phytocassane BGC was found in *Leersia perrieri* and *Zizania latifolia*, which are species belonging to the Oyrzeae tribe, and in several *Oryza* species, indicating that the BGC was obtained by their common ancestor (Miyamoto et al., 2016; Yan et al., 2022).

In this study, we focused on the biosynthesis of oryzalactone to address the acquisition process of novel phytoalexins. The genes involved in the biosynthesis of diterpenoids are highly conserved within rice cultivars. However, as oryzalactone is accumulated in only three of the 69 WRC cultivars (Kariya et al., 2020), its biosynthetic genes are assumed to be cultivar-specific. Thus, analyzing the biosyntheses of these phytoalexins may provide a unique opportunity to address the generation of a biosynthetic pathway, as well as the structural diversification of a group of specialized metabolites. We isolated and characterized the gene responsible for the formation of the oryzalactone carbon skeleton, after which the evolutionary trajectory of the gene was deduced from the distribution of the gene in the species of the genus *Oryza*.

RESULTS

KSLX-OL was identified as a candidate gene responsible for oryzalactone accumulation

Kariya et al. (2020) reported the presence of oryzalactone-accumulating and -lacking chemotypes in rice cultivars. In WRC, only three cultivars, WRC42, WRC47, and WRC68, exhibited oryzalactone accumulation. Thus, we predicted that the causal gene of the specific accumulation of oryzalactone was present in the region close to the single-nucleotide polymorphisms (SNPs) that were specifically detected in the three cultivars. The short-read whole-genome sequencing (WGS) data from the cultivars in WRC (Tanaka et al., 2020) were mapped to the *O. sativa* cv. Nipponbare genome (Os-Nipponbare-Reference-IRGSP-1.0) (Kawahara et al., 2013). Seventeen SNPs that were specific to the three cultivars were detected in the regions around 5.90 Mb on the short arm of chromosome 10 (Chr10-S), 6.65 Mb on the short arm of chromosome 11 (Chr11-S), and 16.4 Mb on the long arm of chromosome 11 (Chr11-L) (Figure 1a; Table S1).

We analyzed the phenotypes and genotypes of the F_2 individuals generated by crossing WRC47, an oryzalactone-accumulating cultivar, and Kasalath, an oryzalactone-lacking cultivar, to clarify the region among Chr10-S, Chr11-S, and Chr11-L that correlated with the oryzalactone-accumulating phenotype. The oryzalactone-accumulating and -lacking phenotypes were segregated in a roughly 3:1 ratio, with 42 of 55 F_2 individuals accumulating oryzalactone (Figure S1a). The genotypes of Chr10-S, Chr11-S, and Chr11-L in the oryzalactone-lacking individuals were determined by PCR-based insertion/deletion analysis (Figure 1b; Figure S1b). The oryzalactone-lacking individuals only exhibited a Kasalath homozygous genotype in the Chr11-L region but exhibited three genotypes (Kasalath homozygous, WRC47 homozygous, and heterozygous) in the Chr10-S region and two genotypes (Kasalath homozygous and heterozygous) in the Chr11-S region. This indicates that the causal gene for the differential accumulation of oryzalactone was in the Chr11-L region.

Thus, we searched the genes around the Chr11-L region using the rice genome annotation database (RAP-DB) and found the *Kaurene Synthase-Like 8* (*KSL8*: Os11g0474800), as well as sequences corresponding to two *KSL8-like* transcripts (Os11g0474583 and Os11 g0474600). As both *KSL8-like* transcripts exhibited high homology to the partial sequences of *KSL8*, the genomic region containing them (Chr11: 16.405–16.416 Mb) was aligned with the exon sequences of *KSL8*, and the entire genomic sequences exhibiting homology with *KSL8* were obtained and defined as *KSL9* (Figure 1a). As *KSL9* and *KSL8* were tandemly arrayed genes, the loci of both genes were defined as *KSL9-KSL8*. *KSL8*s in cv. Nipponbare (*KSL8-jap*) and the indica subspecies (*KSL8-ind*) encode

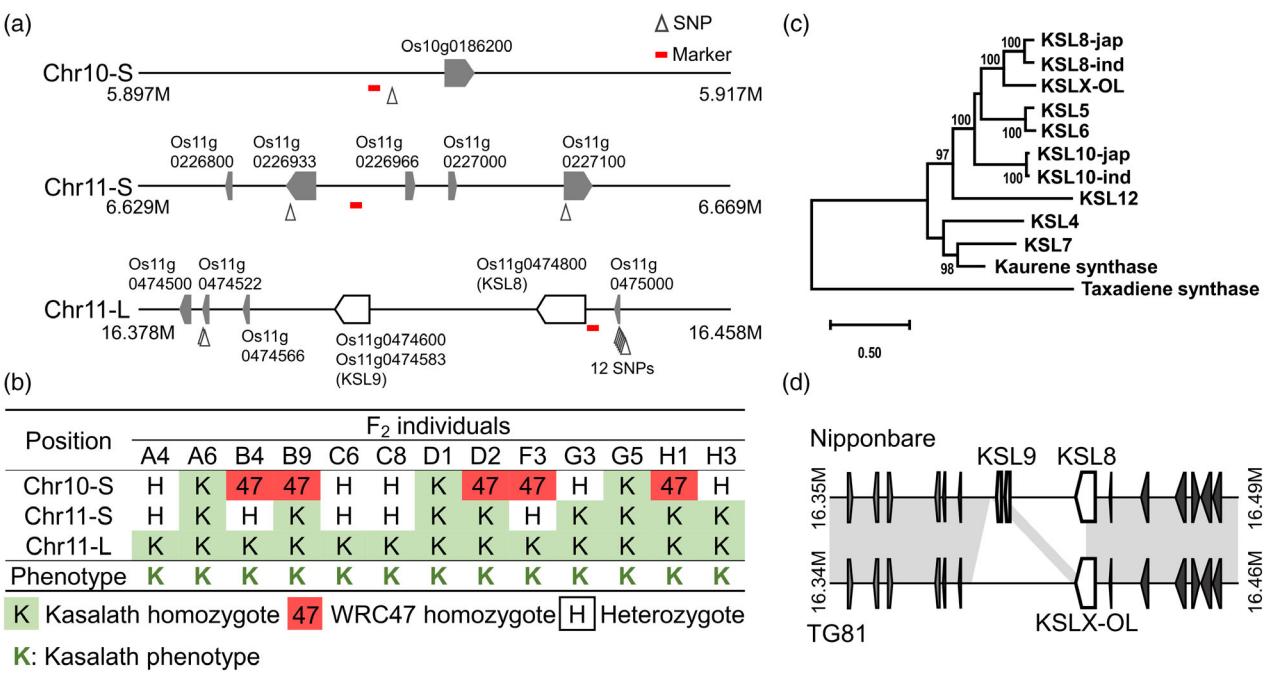

Figure 1. Locus of the oryzalactone biosynthesis gene. (a) Position of the SNPs specific to oryzalactone-accumulating cultivars. Open triangles indicate the positions of specific SNPs and bars indicate the regions used as markers for genotyping. (b) Chr10-S, Chr11-S, and Chr11-L genotypes in F_2 individuals that lack oryzalactone accumulation. (c) Phylogenetic tree of rice KSLs amino acid sequences. jap, japonica; ind, indica. Only ultrafast bootstrap values >95% are shown. (d) Regions around Chr11-L of cv. Nipponbare and cv. TG81.

stemar-13-ene synthase (Nemoto et al., 2004) and stemod-13-ene synthase (Morrone et al., 2006; Toyomasu et al., 2016), respectively, and *KSL9* is a pseudogene (Sakamoto et al., 2004). However, stemar-13-ene and stemod-13-ene were not considered oryzalactone intermediates because of the difference in the carbon skeleton from oryzalactone.

Therefore, we assumed the presence of a different version of *KSL8* in the oryzalactone-accumulating cultivars as the TASUKE database (https://ricegenome-corecollection.dna.affrc.go.jp/) confirmed the presence of the sequences corresponding to exons 1–3 of *KSL8* in WRC42, WRC47, and WRC68 but not for the sequences corresponding to the remaining part of *KSL8*. To explore the *KSL8*-like gene in the oryzalactone-accumulating cultivars, we performed *de novo* assembly using short-read WGS data for WRC47 deposited to the DDBJ Sequence Read Archive by Tanaka et al. (2020), obtaining 387 312 scaffolds. A BLAST search on the scaffolds using the coding sequence (CDS) of *KSL8-jap* as the query found a scaffold exhibiting homology to *KSL8-jap* (15 929 bp). The exon sequences of the *KSL8*-similar gene were estimated by aligning the scaffold and CDS of *KSL8-jap*. Finally, we performed PCR amplicon sequencing as well as the 3′- and 5′-rapid amplification of cDNA ends (RACE) using the total RNA extracted from the UV light-irradiated cv. WRC47 leaves, identifying the full-length CDS of the gene. The identical sequences were also obtained from the total RNA of cv. WRC42 and cv. WRC68 (Figure S2).

Thereafter, we compared these sequences with those of *KSL8-jap* and *KSL8-ind* and confirmed that their homologies were each 82% (Figure S2). Owing to the large differences in the amino acid sequences coded by this CDS and *KSL8*, we named the newly isolated gene *KSLX-OL*. The phylogenetic analysis of the amino acid sequence of KSLX-OL with that of other rice kaurene synthases indicated that KSLX-OL is a sister group of KSL8-jap and KSL8-ind (Figure 1c). The BLAST search indicated that *KSLX-OL* was not present in the cv. Nipponbare genome. Zhang et al. (2022) obtained WGS data from the long and short-reads of 111 rice cultivars and constructed chromosome-level scaffolds through *de novo* assembly. We performed a BLAST search on the available genomic sequences of 82 cultivars and found *KSLX-OL* on chromosome 11 of cv. TG81. A comparison of the chromosome 11 sequences of the two cultivars, Nipponbare and TG81, revealed that *KSL9-KSL8* and *KSLX-OL* are allelic (Figure 1d; Figure S3).

KSLX-OL is a *syn*-abieta-7,12-diene synthase and contributes to oryzalactone biosynthesis

Most rice diterpenoids are synthesized via a two-step enzymatic reaction catalyzed by CPSs and KSLs (Toyomasu et al., 2020). The oryzalactone biosynthetic pathway has been predicted (Figure 2a) based on the stereochemistry of oryzalactone. The orientations of the proton at position 5 and the methyl group at position 20 are α and β in oryzalactone, respectively (Kariya et al., 2020). *Syn*-CPP, which is synthesized by CPS4, exhibits the same conformation at these positions (Otomo et al., 2004; Xu et al., 2004). From the oryzalactone carbon skeleton, we presumed that *KSLX-OL* synthesized *syn*-abieta-7,12-diene using *syn*-CPP as a substrate (Figure 2a).

Next, we characterized the *KSLX-OL*-catalyzed reaction with *syn*-CPP as a substrate. The Agrobacterium strains that harbored *35Spro:CPS4* or *35Spro:KSLX-OL* were co-infiltrated into the leaves of *Nicotiana benthamiana*. After 5 days of incubation, the compounds in the leaves were extracted by *n*-hexane, and the extract was subjected to gas chromatography–mass spectrometry (GC–MS) analysis (Figure 2b). Compounds **1** (r.t. 17.8 min) and **2** (r.t. 18.6 min) were detected in the extract from the leaves co-expressing CPS4 and KSLX-OL (Figure 2b), but not in the negative controls co-expressing CPS4 and green fluorescent protein (GFP), and GFP and KSLX-OL. Compounds **1** and **2** were assumed to be diterpenes based on their mass spectra (Figure 2c), although no candidate compounds were found through a similarity search on the relevant databases. We purified compound **1** from the *N. benthamiana* leaves and identified it as *syn*-abieta-7,12-diene via NMR analyses (Figure S4, Table S2). Compound **2** could not be identified because of its low accumulation.

To examine the enzymatic activity of *KSLX-OL* in rice plants, we constructed an *OsACTpro:KSLX-OL* plasmid by connecting *KSLX-OL* from cv. WRC47 to the downstream rice *actin* promoter and introduced it to the oryzalactone-lacking cultivar, Nipponbare, through Agrobacterium-mediated transformation. After confirming the introduction of *KSLX-OL* into the T_2 transformant generation by PCR, the leaves of the transformants were UV light irradiated for 10 min and incubated for 72 h. A marked accumulation of oryzalactone was detected in the *KSLX-OL*-overexpressing plants (Figure 2d). The amount of oryzalactone in the transgenic plants ranged between 21.7 and 119.4 nmol g^{-1} FW, which was 0.5- to 2.5-fold of the amount detected in the UV-irradiated leaves of cv. WRC47 (Kariya et al., 2020).

KSLX-OL and its allele, *KSLX-NOL*, are present in *Oryza sativa* and *Oryza rufipogon*

The relationship between the presence of *KSLX-OL* and oryzalactone accumulation was examined in the 69 WRC cultivars and 30 strains of *O. rufipogon* (Kajiya-Kanegae et al., 2021), a closely related ancestral relative of *O. sativa*.

The reference sequence of *KSLX-OL* was obtained from the cv. TG81 genome and those of *KSL8* and *KSL9* were obtained from the cv. Nipponbare genome. As the homologies between the exons of three *KSL*s were higher than 77% in each case, we simultaneously mapped the WGS data to the concatenated sequences of *KSL8*, *KSL9*,

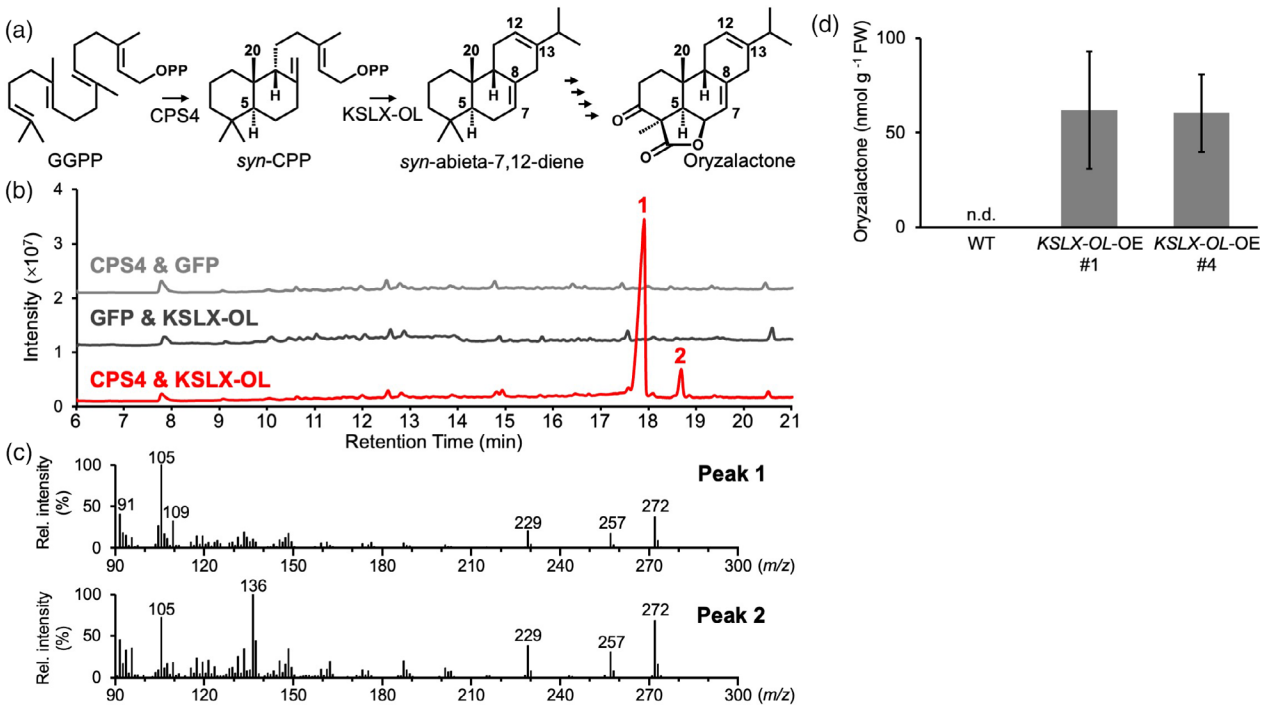

Figure 2. Functional analysis of KSLX-OL. (a) Hypothetical pathway of oryzalactone biosynthesis. (b) Total ion current chromatogram of GC–MS analysis of the extracts obtained from tobacco leaves co-expressing CPS4 and GFP (gray, negative control), GFP and KSLX-OL (black, negative control), and CPS4 and KSLX-OL (red). (c) Mass spectra of peaks 1 (r.t. 17.8 min) and 2 (r.t. 18.7 min) detected from the extract of tobacco leaves co-expressing CPS4 and KSLX-OL (red line in b). (d) Accumulated amount of oryzalactone in the *KSLX-OL*-overexpressing mutant strains. Oryzalactone accumulation was examined for at least eight individuals from each of two independent strains. Values are presented as the mean ± standard error. WT, wild type; OE, overexpression; n.d., not detected.

and *KSLX-OL* to avoid mis-mapping. We obtained the assembled *KSLX-OL* sequences from the WRC cultivars and *O. rufipogon* strains.

We performed principal component analysis (PCA) using the assembled *KSLX-OL* sequences of the WRC cultivars and *O. rufipogon* strains (Figure 3a; Table S3). The first principal component was strongly associated with the proportion of gaps in the assembled *KSLX-OL* sequences. The percentage of gaps in the cultivars grouped in the upper-right region was greater than 48%, whereas that in the cultivars in the left region was less than 26%; thus, we regarded the former and latter as the *KSLX-OL*-lacking and -possessing strains, respectively. To confirm the absence of sequences that are homologous to *KSLX-OL* in the *KSLX-OL*-lacking strains, we performed *de novo* assembly using the short-read WGS data from a *KSLX*-lacking cultivar, WRC11. The BLAST search on the obtained scaffolds using CDS of *KSLX-OL* as a query failed to detect *KSLX-OL*, indicating the absence of *KSLX-OL*-like sequences in the strains that were classified as *KSLX-OL*-lacking strains.

The *KSLX-OL*-possessing strains included the oryzalactone-accumulating and lacking strains (Kariya et al., 2020). To clarify the relationship between the assembled *KSLX-OL* sequences and oryzalactone accumulation, we constructed a phylogenetic tree based on the amino acid sequences inferred from the nucleotide sequences that are homologous to the *KSLX-OL* exon region in the assembled *KSLX-OL* sequences from the *KSLX-OL*-possessing strains. The sequences were divided into two clades: the *KSLX-OL* sequences that were mainly from the oryzalactone-accumulating and oryzalactone-lacking strains (Figure 3b, Kariya et al., 2020). Thus, we redefined the sequences in the latter clade as *KSLX-NOL* (*KSLX* in non-oryzalactone-producing strains). To examine the enzymatic activity of *KSLX-NOL*, we cloned *KSLX-NOL* from cv. WRC22 and co-expressed with *CPS4* in *N. benthamiana* leaves and detected the accumulation of **3** in the leaves through GC–MS analysis (Figure S5). The compound was expected to be a diterpene based on its mass spectrum, although its chemical structure was not determined by searching the relevant databases. The mass spectrum of **3** differed from those of the compounds generated by KSLX-OL, KSL8-jap, and KSL8-ind from *syn*-CPP (Figure 2c; Toyomasu et al., 2018). Thus, KSLX-NOL catalyzes a different reaction from those of these three KSLs.

KSLX-possessing strains lack *KSL9-KSL8* in *Oryza sativa* and *Oryza rufipogon*

Further, the assembled sequences of *KSL8* and *KSL9* in the WRC cultivars and *O. rufipogon* strains were subjected to PCA (Figure 3c,d). The sequences of *KSL8* were divided into three groups, that is, *KSL8-jap*, *KSL8-ind*, and the sequences

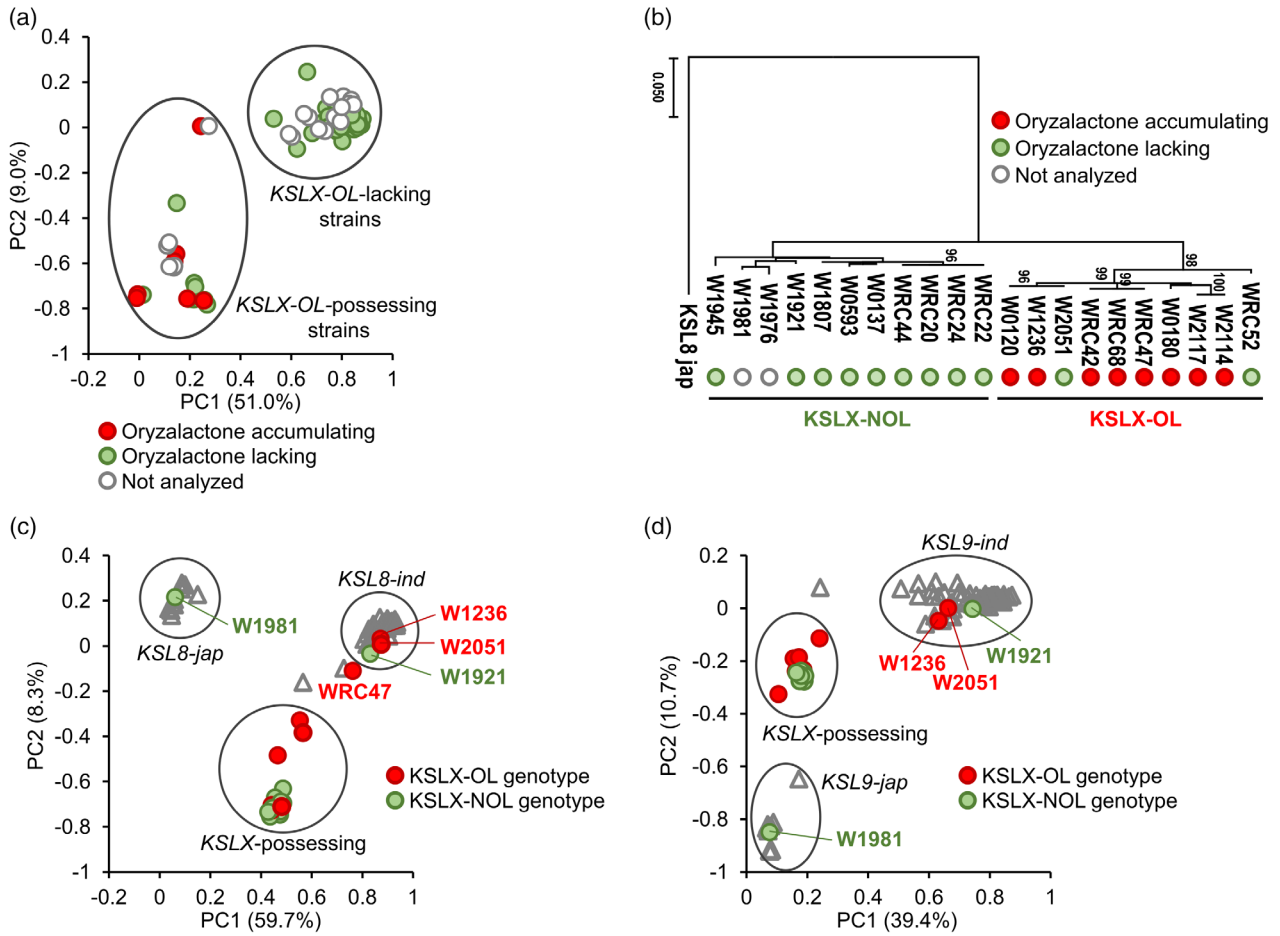

Figure 3. Distribution of *KSLX*, *KSL8*, and *KSL9* in the 69 WRC cultivars and 30 strains of *O. rufipogon*. Principal component analysis of the *KSLX-OL*-assembled sequences (a) and phylogenetic tree generated with the amino acid sequences of KSLX-OLs in the *KSLX-OL*-possessing strains (b). Red and green circles indicate the oryzalactone accumulating and lacking phenotypes, respectively. Principal component analysis of assembled *KSL8* (c) and *KSL9* (d) in WRC cultivars and *Oryza rufipogon* strains. Red and green circles indicate the *KSLX-OL* and *KSLX-NOL* genotype, respectively, and triangle indicates *KSLX*-lacking genotype. WRC, World Rice Core collection; W, wild rice, *Oryza rufipogon*.

from *KSLX*-possessing strains (Figure 3c). Put differently, the analyzed strains were classified into three groups based on the differences in their *KSL8* sequences. The *KSL9* sequences were also divided into three groups by PCA (Figure 3d). One group corresponded to the sequences from the *KSLX*-possessing strains. The remaining two groups corresponded to the *KSL9* sequences from the strains containing *KSL8-jap* and *KSL8-ind*; thus, we named the respective *KSL9* sequences as *KSL9-jap* or *KSL9-ind*. The average percentage of gaps within the *KSL8*- and *KSL9*-assembled sequences from the genomic data of the *KSLX*-possessing strains were 40.3% and 64.2%, respectively, indicating that *KSL8* and *KSL9* could not be assembled in the *KSLX*-possessing strains. The partial assembly in these strains was attributable to the presence of highly similar sequences between the *KSLX*, *KSL8*, and *KSL9* and to the presence of interspersed repetitive sequences in the reference sequences of the genes. This finding further supports the assignment of *KSLX* as an allele of *KSL9-KSL8*, which is consistent with the comparison of the chromosome 11 sequences between the *KSLX-OL*-possessing and *KSL9-KSL8*-possessing strains (Figure 1d).

However, four *KSLX*-possessing *O. rufipogon* strains, W1981, W1236, W1921, and W2051, were exceptions as they also possessed *KSL8* and *KSL9* (Figure 3c,d). Thus, we expanded the analysis to the assembled *KSL*s from the WGS data of 445 *O. rufipogon* strains and confirmed that the *O. rufipogon* strains were classified into the *KSLX*-possessing (29.2%), *KSL8-KSL9*-possessing (56.2%), and minor *KSL8-KSL9-KSLX*-possessing strains (14.6%) (Figure S6, Table S4). This finding indicated that the *KSL8-KSL9-KSLX*-possessing strains are widely spread in *O. rufipogon*. To address the origin of the *KSL8-KSL9-KSLX*-possessing strains, we generated a phylogenetic tree based on *KSLX* intron sequences for more sensitive analysis (Figure S7a). The *KSLX* intron sequences in W1236 and W2051 were

included in the *KSLX-OL* clade, whereas W1921 and W1981 were in the *KSLX-NOL* clade, and this is consistent with the phylogenetic analysis based on *KSLX* exon sequences (Figure 3b). Similarly, a phylogenetic tree of the *KSL8* intron sequences indicated that the *KSL8* sequence in W1981 was in the *KSL8-jap* clade, whereas those in W1236, W1921, and W2051 were in the *KSL8-ind* clade (Figure S7b). These findings indicated that *KSLX* and *KSL8* in the *KSL8-KSL9-KSLX*-possessing strains were phylogenetically related to those in the *KSLX*- and *KSL8-KSL9*-possessing strains, respectively. Thus, the *KSL8-KSL9-KSLX* genotype may have been secondarily generated from the *KSL9-KSL8* and *KSLX* genotypes (Figure S7c).

KSLX was widely distributed in the AA genome species

The CDSs of the KSLs in *O. sativa* (AA genome), *O. punctata* (BB genome), *O. brachyantha* (FF genome), *Leersia perrieri*, *Zea mays*, *A. thaliana*, and *Physcomitrella patens* from the Gramene database were subjected to phylogenetic analysis to elucidate the distribution of *KSL8* and its allelic genes in plants (Figure S8). Homologs of *KSL8*, *KSL9*, and *KSLX* were only observed in *O. punctata* and *O. brachyantha*; thus, we assumed that the *KSL8* homologs specifically evolved in the genus *Oryza*.

Subsequently, we analyzed the distributions of *KSLX*, *KSL8*, and *KSL9* in the genus *Oryza*. The distribution of *KSLX* was analyzed using the WGS data from 282 strains of 21 *Oryza* species. The WGS data were mapped to the reference *KSLX-OL* sequence, and the obtained sequences were subjected to PCA (Figure 4a). The first principal component represented the percentage of gaps in the analyzed sequences. Although the strains in the right region displayed a large percentage of gaps, the *KSLX*-possessing strains in *O. sativa* and *O. rufipogon* were located in the left region. Thus, the groups on the left and right were designated as the *KSLX*-possessing and -lacking strains, respectively. Thus, *KSLX* was assumed to be a gene that is specific to the AA genome species as only the AA genome species were included in the *KSLX*-possessing group. The *KSLX* sequences in the *KSLX*-possessing group were divided into three groups, *KSLX-OL*, *KSLX-NOL*, and *KSLX-bar* (*KSLX*s in *O. barthii* and *O. glumaepatula*), via phylogenetic analysis (Figure 4b). The distributions of *KSL8* and *KSL9* in the AA, BB, and FF genome species were analyzed by the BLAST search using the Gramene database. The genes exhibiting high homology with *KSL8* were detected in all the analyzed species; however, *KSL9* was only detected in the AA genome species (Figure S9).

KSLX is a fusion gene derived from *KSL8* and *KSL9*

The phylogenetic analysis using the exon sequences of *KSL8*s, *KSL9*s, and *KSLX*s in the AA, BB, and FF genome species indicated that *KSLX* and *KSL9* were phylogenetically related, whereas *KSL8* was distant from *KSLX* and *KSL9* (Figure S10). However, the comparison of the sequences of chromosome 11 between cv. Nipponbare and cv. TG81 (Figure 1d) indicated that a closer relationship between *KSLX* and *KSL9* was not true for the entire gene sequence and that the 5′-end side of *KSLX* was closely related to that of *KSL8*. For confirmation, the *KSL*s were divided into individual exons and introns, and phylogenetic analysis was performed separately for each region (Figure S11). The phylogenetic relationships of the sequences corresponding to exon 5 to intron 6 of *KSL8* were not analyzed because of the lack of sequences in *KSL9*s. *KSLX* and *KSL8* tended to be closely related in the region from exon 1 to intron 3, whereas *KSLX* and *KSL9* tended to be closely related in the region from exon 4 to 13. The phylogenetic analysis using exon 1 to intron 3 as the 5′-end region and exon 4–13 as the 3′-end region demonstrated the same tendency with high confidence (Figure 5). Additionally, the 5′- and 3′-flanking regions of *KSLX* exhibited high sequence similarity with those of *KSL8* and *KSL9*, respectively, in *O. sativa* (Figure S3). These findings indicate that *KSLX* is a fusion gene derived from ancestral *KSL8* and *KSL9*.

Oryzalactone and oryzalexin S exhibited similar antimicrobial activities

We compared the antimicrobial activities of oryzalactone and oryzalexin S, which are the phytoalexins produced by KSLX-OL and KSL8-jap, respectively (Table 1, Figure S12). The half-maximal inhibitory concentration (IC_{50}) values for the inhibition of the conidial germination of four *Pyricularia oryzae* strains were greater than 785 μM for oryzalactone, whereas those for oryzalexin S were 63.9–153 μM. Thus, oryzalexin S exhibited a stronger inhibitory activity against the conidial germination of *P. oryzae*. However, both compounds remarkably inhibited the germ tube elongation of *P. oryzae* at lower concentrations, and the IC_{50} values of oryzalactone and oryzalexin S were in the ranges of 19.9–98.5 and 29.3–236 μM, respectively. Oryzalactone and oryzalexin S at 1000 μM exhibited a slight inhibitory activity on the conidial germination of *Bipolaris oryzae*, the causal agent of rice brown spot, whereas the compounds inhibited the germ tube elongation at lower concentrations, with IC_{50} values of 42.4 and 71.5 μM, respectively. None of the compounds inhibited the growth of the rice pathogenic bacteria, *Xanthomonas oryzae* and *Burkholderia glumae*, at 1000 μM.

DISCUSSION

In this study, we elucidated the genetic factor that accounts for the accumulation of oryzalactone, a rice cultivar-specific phytoalexin. We identified a candidate gene for oryzalactone accumulation, *KSLX-OL*, through SNP analysis. The functional analyses of KSLX-OL in *N. benthamiana* and the rice cultivar Nipponbare, which accumulates momilactone

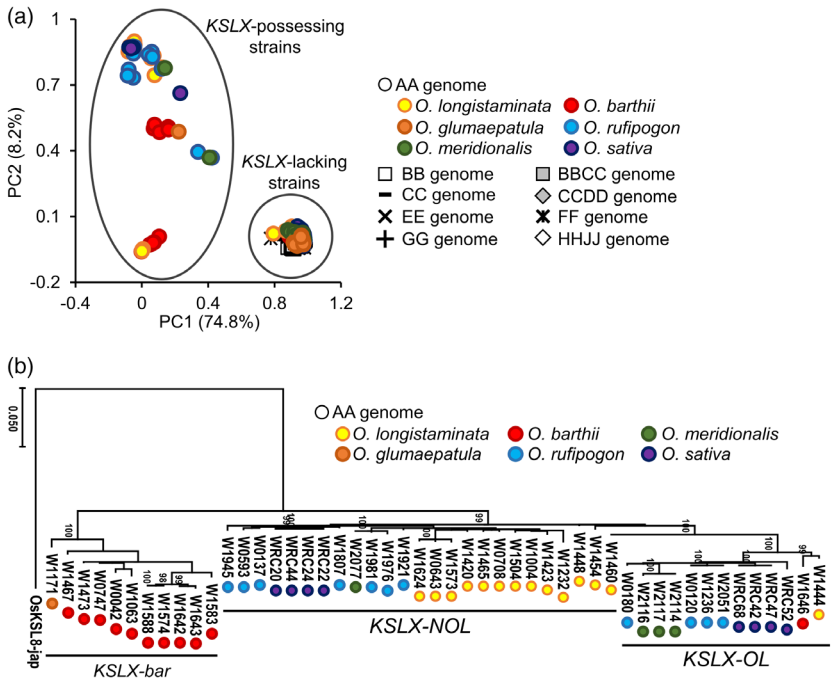

Figure 4. Distribution of *KSLX* in the genus *Oryza*. (a) Principal component analysis of *KSLX-OL* coding sequences in the genus *Oryza*. (b) Phylogenetic tree of *KSLX*s in the *KSLX*-possessing strains in the genus *Oryza*. The phylogenetic tree was generated based on the nucleotide sequences. WRC, World Rice Core collection; W, wild rice species.

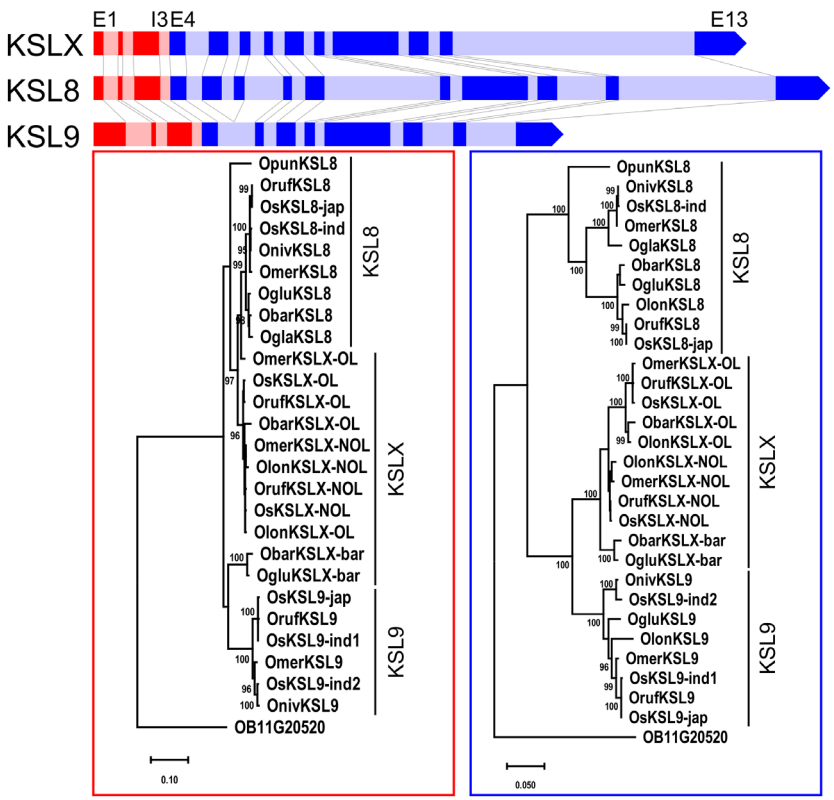

Figure 5. Phylogenetic tree of *KSL8*, *KSL9*, and *KSLX* in the AA genomic species from exon 1 to intron 3 (E1–I3, red), and from exon 4 to 13 (E4–E13, blue).

Table 1 IC_{50} values of oryzalactone and oryzalexin S for the inhibition of conidial germination and germ tube elongation of *Pyricularia oryzae* and *Biopolaris oryzae* and for growth inhibition of *Xanthomonas oryzae* and *Burkholderia glumae*

	Conidial germination				
	P. oryzae 101447 μM	*P. oryzae* 101001 μM	*P. oryzae* 101519 μM	*P. oryzae* naga69-150 μM	*B. oryzae* μM
Oryzalactone	785	>1000 (26)	>1000 (48)	916	>1000 (17)
Oryzalexin S	63.9	153	67.8	74.7	>1000 (21)
	Germ tube elongation				
	P. oryzae 101447 μM	*P. oryzae* 101001 μM	*P. oryzae* 101519 μM	*P. oryzae* naga69-150 μM	*B. oryzae* μM
Oryzalactone	19.9	23.6	47.0	98.5	42.4
Oryzalexin S	29.3	63.5	38.0	236	71.5
			Bacterial growth		
			X. oryzae μM		*B. glumae* μM
Oryzalactone			>1000 (0)		>1000 (0)
Oryzalexin S			>1000 (0)		>1000 (6)

The values in parentheses are inhibition rates (%) at 1000 μM.

A but not oryzalactone, indicated that the gene, *KSLX-OL*, accounts for oryzalactone biosynthesis and that the oryzalactone biosynthetic pathway was generated by *KSLX-OL* acquisition (Figure 2).

Diversification of *KSLs* results in diterpenoid phytoalexin biosynthetic pathway diversity

We isolated two *KSLX-OL* homologs: *KSLX-NOL* from oryzalactone-lacking strains and *KSLX-bar* from *O. barthii* and *O. glumaepatula*, and they exhibited 96.2% and 92.9% homologies with *KSLX-OL*, respectively. The transient expression in *N. benthamiana* indicated that *KSLX-NOL* is a diterpene synthase that cyclizes *syn*-CPP (Figure S5). It was predicted that *KSLX-bar* functions as a diterpene synthase because it contains two motifs, DDxxD and NSE/DTE, that are conserved in diterpene synthases (Chen et al., 2011). Thus, it is plausible that *KSLX-NOL* and *KSLX-bar* are involved in the biosynthesis of uncharacterized diterpenoid phytoalexins.

The homologies between *KSL8-jap* and *KSL8-ind*, as well as between *KSLX-OL* and *KSLX-NOL*, were greater than 90.0%, although each of these enzymes catalyzes different reactions (Toyomasu et al., 2016). Previous reports reveal that diterpene synthases change products through a small number of mutations (Morrone et al., 2008; Xu, Wilderman, & Peters, 2007). This plasticity of KSLs facilitates the emergence of a gene that encodes for an enzyme with a new function, resulting in the increased diversity of the carbon skeleton of diterpenoids. More than 15 diterpenoids are reported as rice phytoalexins (Kariya et al., 2023; Valletta et al., 2023). This diversity is related to the ability of diterpene synthases to produce a wide variety of carbon skeletons.

The presence of oxidative metabolic pathways that can accept a wide range of diterpene carbon skeletons is another factor that enables the diversification of rice diterpenoid phytoalexins. The acquisition of new genes may be accompanied by the generation of new metabolites that cause autotoxicity. For example, the retention of the incomplete momilactone biosynthetic pathway, that is, the lack of CYP76M7/8, causes a lesion mimic phenotype in rice (Li et al., 2021). The oxidation of secondary metabolites is key to reducing autotoxicity. As the oxidation patterns of oryzalactone and momilactone A are the same, the oxidases, CYP99A2/3, CYP76M7/8, OsMS1/2, and CYP701A8, that function in the momilactone A biosynthesis pathway (Kitaoka et al., 2021) are presumably involved in oryzalactone biosynthesis. Thus, the oryzalactone biosynthetic pathway could have been generated to avoid the accumulation of toxic intermediates by diverting the biosynthetic enzymes to generate different phytoalexins. Similar examples have been reported in the biosynthetic pathways of other rice phytoalexins. Although *CYP99A2/3* and *CYP71Z21/22* are the genes in momilactone and *ent*-10-oxodepressin BGCs, respectively, they are also involved in oryzalexin S biosynthesis (Zhao et al., 2023). Thus, the presence of an oxidative pathway that can accept a wide range of substrates is considered a preadaptation step for creating new biosynthetic pathways in the diversification of rice diterpenoid phytoalexins.

KSLX was generated through gene duplication, functional differentiation, and gene fusion

We hypothesized the process of *KSLX* acquisition (Figure 6). We anticipated that the ancestral *KSL8* (*ancKSL8*) and *KSLY*, the most recent common ancestor (MRCA) of *KSL9* and *KSLX*, would be generated by the duplication of *mrcaKSL* (MRCA of *KSL8*, *KSL9*, and *KSLX*) as *KSL8*s were the sister groups of *KSL9*s and *KSLX*s (Figure 5; Figure S10). The duplication of *mrcaKSL* presumably proceeded after the diversification of the FF genome species as the *KSL8* homolog in *O. brachyantha* (FF), OB11G20520, was an outgroup of *KSL8*s, *KSL9*s, and *KSLX*s in the AA and BB genome species (Figure 5; Figure S10). *KSL8*s in the AA genome species form a distinct clade together with *KSL8* in *O. punctata* (BB) separately from the clade containing *KSLX*s and *KSL9*s in the phylogenetic tree generated using exon 4–13 (Figure 5; Figure S11). This topology indicated that the *mrcaKSL* duplication leading to the generation of *KSLY* and *KSL8* was occurred before AA-BB splitting (Figure S13). Because neither *KSL9* nor *KSLX* are present in *O. punctata*, the *KSLY* was likely eliminated in the lineage to the BB genome species. The functional differentiation of *KSLY* into ancestral *KSL9* (*ancKSL9*) and *KSLX* (*ancKSLX*) may have occurred in the lineage to the AA genome species. *OpKSL8* was an outgroup of *KSLX* and *KSL8* in the phylogenetic analysis of the 5′-end side sequences of *KSLX*, *KSL8*, and *KSL9* in the AA genome (Figure 5). These findings indicated that *KSLX*s in the AA genome species were derived by fusing *ancKSL8* and *ancKSLX*, and this gene fusion occurred after the AA-BB splitting. As *KSLX-OL* and *KSLX-NOL* are widely distributed in the AA genome species, the functional differentiation of KSLX likely occurred before speciation in the AA genome.

We observed that four *O. rufipogon* strains, W1981, W1236, W1921, and W2051, exhibited the *KSL8-KSL9-KSLX* genotype. Employing phylogenetic analysis, we found that *KSLX*s in the *KSL8-KSL9-KSLX* genotype strains were divided into *KSLX-OL* and *KSLX-NOL* groups (Figure S7a). Thus, it is unlikely that *KSLX*s in these strains were derived from the common ancestor of *KSLX-OL* and *KSLX-NOL* in the *KSLX* genotype strains. Similarly, *KSL8*s in these strains were divided into *KSL8-ind* and *KSL8-jap* (Figure S7b). Thus, *KSL8*s in these strains were considered not derived from the common ancestors of *KSL8-ind* and *KSL8-jap* in the *KSL9-KSL8* genotype strains. These indicate that the *KSL8-KSL9-KSLX* genotype may not have originated from the tandem duplication that generated the fused gene, *KSLX*. Furthermore, the various combinations of the *KSL8* and *KSLX* subgroups were observed in the strains with the *KSL8-KSL9-KSLX* genotype (W1236 and W2051: *KSL8-ind–KSLX-OL*, W1921: *KSL8-ind–KSLX-NOL*, and W1981: *KSL8-jap–KSLX-NOL*). The simplest explanation for this pattern is that the *KSL8-KSL9-KSLX* genotype was generated by the secondary incorporation of *KSLX* after the establishments of the *KSLX-OL* and *KSLX-NOL*

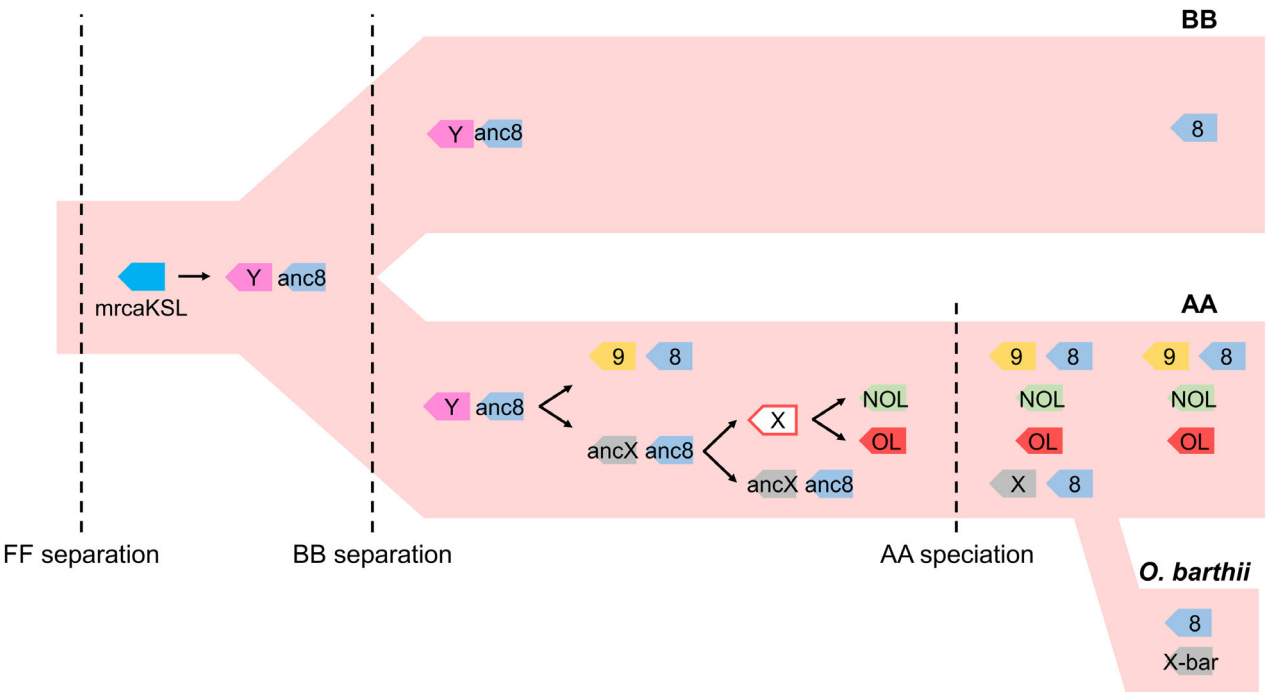

Figure 6. Hypothetical process of acquisition and diversification of *KSL8*, *KSL9*, and *KSLX*. 8, *KSL8*; 9, *KSL9*; X, *KSLX*; Y, *KSLY*; OL, *KSLX-OL*; NOL, *KSLX-NOL*; X-bar, *KSLX-bar*; anc, ancestor; mrca, most recent common ancestor.

subgroups and *KSL8-ind* and *KSL8-jap* subgroups (Figure S7c).

KSLX-bar was phylogenetically distinct from *KSLX-OL* and *KSLX-NOL* (Figure 4b). The phylogenetic analysis revealed that the 5′-end side of *KSLX-bar* was a sister group of *KSL9* (Figure 5), indicating that *KSLX-bar* was derived from *ancKSLX* without the gene fusion between *ancKSLX* and *ancKSL8* observed in the creation of *KSLX-OL* and *KSLX-NOL* (Figure 6).

Plants accumulate a vast number of diverse secondary metabolites; however, only a few studies have demonstrated the diversification processes of metabolic pathways. In this study, we demonstrate the diversification process of diterpenoids through the creation of a new gene by the duplication and functional differentiation of a biosynthetic gene. Kliebenstein, Lambrix, et al. (2001) reported that duplicated genes conferred the structural diversity of glucosinolates in *A. thaliana*. The oxidation of the glucosinolate side chain is regulated by two 2-oxoglutarate-dependent dioxygenases, AtAOP2 and AtAOP3, which were derived from a common ancestor. The AOP2-expressing strains accumulate alkenyl-type glucosinolates, whereas the AOP3-expressing strains accumulate hydroxyalkyl-type glucosinolates.

Furthermore, we observed that a gene fusion event occurred during the evolutionary process of *KSLX*. It has been demonstrated that gene fusion is an important factor in the acquisition of new phenotypes through the neofunctionalization of genes (Zhou et al., 2022). In the case of *KSLX*, the active center was derived from *ancKSLX*, whereas the *N*-terminal region of the protein and promoter sequences controlling gene expression were derived from *ancKSL8*. However, the direct effect of gene fusion on *KSLX* function is unclear, although slight changes in the steric conformation of the protein caused by the fusion of the *N*-terminal region of *ancKSL8* might have affected the enzymatic activity. Additionally, the changes in the copy number and gene expression patterns might have affected its function through evolutionary processes, such as the retention of accumulated mutations, that allow for efficient phytoalexin biosynthesis.

KSLX and *KSL9-KSL8* may have been undergoing balancing selection

According to the inferred *KSLX* acquisition process, an allelic polymorphism at the *KSL9-KSL8/KSLX* locus was present before the speciation of the AA genome (Figure 6). One explanation for this long-term coexistence of allelic polymorphism is the balancing selection. The genome-wide analyses of *A. thaliana* and *Capsella* demonstrated that genetic diversity is high at the defense-related loci (Goktay et al., 2020; Koenig et al., 2019), indicating that the balancing selection of defense-related genes is common in plants (Goktay et al., 2020). Additionally, in *A. thaliana*, the alleles for MAM2 that control the length of glucosinolate side chains are assumed to have undergone balancing selection due to their interactions with herbivores (Kroymann et al., 2003; Zust et al., 2012). As the major roles of specialized metabolites are considered related to defense responses, the maintenance of multiple chemotypes through balancing selection is reasonable, although our knowledge of similar examples is limited.

The changes in the fitness of allelic traits with time and location result in balancing selection. Thus, we examined the possibility of oryzalactone and oryzalexin S exhibiting different antimicrobial spectra. Assuming this is true, the fitness of these chemotypes would vary with the selection pressure by the endemic diseases. The IC_{50} values of oryzalexin S on the inhibition of the conidia germination of *P. oryzae* were lower than those of oryzalactone. The stronger antifungal activity of oryzalexin S on *P. oryzae* might have contributed to the spreading of the chemotype to respond to the selective pressure from the pathogen (Table 1; Figure S12). Rice diterpenoid phytoalexins exhibit diverse biological activities. The accumulation of diterpenoid phytoalexins affects the resistance to the root-knot nematode, *Meloidogyne graminicola*, and the ratio of the nematode species, such as *Acrobeloides* and *Meloidogyne*, in the rice roots and its rhizosphere (Desmedt et al., 2022). Lu et al. (2018) reported that the rhizosphere microbiota in phytoalexin-deficient rice mutants was altered. *KSLX-OL* and *KSL8-jap* were constitutively expressed in the roots of cv. WRC47 and cv. Nipponbare, respectively (Figure S14), indicating that oryzalactone and oryzalexin S were also produced in the roots. Considering the multifaced functions of rice diterpenoid phytoalexins, the differences in the biological activities other than antimicrobial activity are possible causal factors of the long-term coexistence of phytoalexin chemotypes.

EXPERIMENTAL PROCEDURES

Plant materials

Cultivar seeds from the WRC (*Oryza sativa* L.) and African rice, *Oryza glaberrima* Steud., were obtained from the NARO Genebank (Tsukuba, Japan). Seeds of wild rice species (*Oryza rufipogon* Griff., *Oryza barthii* A. Chev., *Oryza glumaepatula* Steud., *Oryza meridionalis* N. Q. Ng, *Oryza punctata* Kotschy ex Steud., and *Oryza brachyantha* A. Chev. Et Rhoer.) were obtained from the National Institute of Genetics (Oryzabase, https://shigen.nig.ac.jp/rice/oryzabase/about/oryzabase, Japan). The F_2 population was generated by crossing cv. WRC47 and cv. Kasalath and was used for the identification of *KSLX-OL*.

Analysis of oryzalactone in rice leaves

Rice seeds were sown in a 1:4 mixture ratio of vermiculite (Shoei Sangyo, Okayama, Japan) and artificial compost for rice (Grin Grow, Okayama, Japan) and grown at 28°C with a 16/8 h light/dark cycle until the third leaves developed. The induction and

quantification of oryzalectone were performed according to previously described methods (Kariya et al., 2020).

Exploring for genomic regions where oryzalactone biosynthesis genes are located

Whole genome sequence data for the WRC (Tanaka et al., 2020) were downloaded from DDBJ Sequence Read Archive. Trimming of raw paired-end reads and the subsequent mapping against Os-Nipponbare-Reference-IRGSP-1.0 (Kawahara et al., 2013) was performed using Galaxy/NAAC, a web-based platform for bioinformatics analysis (https://galaxy.dna.afrc.go.jp/nias/static/register_en.html). The construction of the genetic map was performed according to a previous study by Yoshida et al. (2022). The SNPs specific to oryzalactone-accumulating cultivars in WRC were extracted and the genomic regions with the cultivar-specific SNPs were named Chr10-S, Chr11-S, and Chr11-L. Randomly selected F_2 individuals ($n = 55$) were grown for 4 weeks. The 3rd to 5th leaves were cut and irradiated with UV light for 10 min, and the accumulation of oryzalactone was analyzed by liquid chromatography with tandem mass spectrometry. The leaf sheath was stored at −80°C until genomic DNA extraction. Extraction of genomic DNA was performed according to a previous study (Kariya et al., 2019). The genotypes of the individuals that exhibited the Kasalath phenotype were determined for the Chr10-S, Chr11-S, and Chr11-L regions by PCR using Insertion/Deletion as markers. The primers used for genotyping are listed in Table S5.

Determination of coding sequence of *KSLX-OL* and *KSLX-NOL*

De novo assembly was performed using MEGAHIT (Li et al., 2015) to explore a *KSL8-like* sequence in cv. WRC47 and cv. WRC11. *KSLX-OL* and *KSLX-NOL* were determined from cv. WRC47 and cv. WRC22, respectively. Rice leaves were irradiated under UV light for 10 min and incubated for 24 h at 28°C to induce the expression of the oryzalactone biosynthetic genes. Total RNA was extracted from the leaves using an RNeasy Plant Kit (Qiagen, Venlo, Netherlands) according to the manufacturer's protocol. The obtained mRNA was used for 3′- and 5′-RACE analysis. The details are described in Method S. The sequences were deposited to DDBJ. Accession ID of *KSLX-OL* and *KSLX-NOL* are LC774656 and LC774657, respectively.

Phylogenetic analysis

The analyzed sequences were aligned by MAFFT (Katoh & Standley, 2013) and trimmed using trimAl (Capella-Gutierrez et al., 2009). Phylogenetic analysis was performed using the Maximum Likelihood method with IQ-TREE2 (Minh et al., 2020). The confidence level of the phylogenetic tree was estimated by UFboot2, and bootstrap values greater than 95% were considered reliable (Hoang et al., 2018). For details on the analyzed sequences, see Method S.

Comparison of chromosome 11 sequences between cv. Nipponbare and cv. TG81

Chromosome-level scaffolds of the 82 strains deposited by Zhang et al. (2022) were obtained from https://cgm.sjtu.edu.cn/TGSrice/index.html. BLAST+ was used to search for *KSLX-OL* and it was found in cv. TG81. The comparison of chromosome 11 sequences of cv. TG81 and cv. Nipponbare was performed using D-GENIES (Cabanettes & Klopp, 2018).

Functional analysis of KSLX-OL in *Nicotiana benthamiana*

To overexpress terpene synthases in *N. benthamiana*, we prepared *35Spro:CPS4*, *35Spro: KSLX-OL*, and *35Spro:KSLX-NOL* in the binary vector pRI201-AN (Takara Bio, Kusatsu, Japan). *KSLX-OL* and *KSLX-NOL* were cloned from cv. WRC47 and cv. WRC22, respectively, and *CPS4* was from cv. Nipponbare. Tomato bushy stunt virus *p19* was co-expressed to suppress post-transcriptional gene silencing. GFP was expressed as the negative control. The *35Spro:p19* and *35Spro: GFP* were used from the stock of the Laboratory of Nutritional Science, Tottori University. The *Agrobacterium tumefaciens* strain GV3101 harboring the overexpression vector was cultured at 25°C in LB medium containing 25 μg ml^{-1} rifampicin, 50 μg ml^{-1} kanamycin, and 50 μg ml^{-1} gentamycin. The culture was centrifuged, and the obtained pellet was suspended in infiltration buffer (Hanano & Goto, 2011). The suspension was injected through the underside of tobacco leaves which grown at 25°C for 4 weeks on a 16/8 h light/dark cycle. The plants were incubated under high humidity conditions for 2 days and then placed under normal growth conditions for 3 days. The leaves were ground with liquid nitrogen and extracted with a 10 vol. equivalent of *n*-hexane. The extract was evaporated, and the residue was subjected to silica gel column chromatography. The eluate was evaporated and resolved in 100 μl *n*-hexane and underwent GC–MS [GCMS-QP2010Plus (Shimadzu, Kyoto, Japan)] analyses. Compound **1** detected in the extract from the leaves co-expressing CPS4 and KSLX-OL was purified and identified to be *syn*-abieta-7,12-diene via NMR analyses (Figures S15–S21). Details are described in Method S1.

Overexpression of *OsKSLX-OL* in rice plants

To create *KSLX-OL*-overexpressing transgenic rice plants, we cloned *KSLX-OL* from cv. WRC47 and ligated it into the pActnos/Hm2 binary vector (Sentoku et al., 2000), which includes the rice *actin* promotor (*OsACTpro*). The linearized plasmid was prepared by PCR using Primestar GXL (Takara Bio). The cloned vector and *KSLX-OL* amplicon were ligated using an In-Fusion cloning kit to obtain *OsACTpro:KSLX-OL*. The constructs were introduced into the *A. tumefaciens* strain EHA105 and transformed into the Nipponbare calli cultivar using the Agrobacterium-mediated transformation method (Hiei et al., 1994). An empty vector was used as a control. The presence of the transgene in each transformant was confirmed via PCR with *KSLX-OL*-specific primers (Table S5).

Distribution of *KSL8, KSL9,* and *KSLX* in the species of genus *Oryza*

The WGS data of the cultivars in the WRC (Tanaka et al., 2020) and that of 217 wild rice strains listed in OryzaGenome2.1 (Kajiya-Kanegae et al., 2021) were obtained from the DDBJ Sequence Read Archive. The accession numbers of the WGS data are summarized in Table S6. The low-coverage WGS data of the *O. rufipogon* strains deposited by Huang et al. (2012) were obtained from the European Nucleotide Archive (ERP001143). The reference sequence of *KSLX-OL*, *KSL9*, and *KSL8* were obtained from the cv. TG81 genome (Zhang et al., 2022) and RAP-DB (https://rapdb.dna.affrc.go.jp/). These sequences were tandemly arrayed, and the WGS data were mapped using BWA-MEM2 (Vasimuddin et al., 2019). Consensus sequences were analyzed by PCA. Details are described in Method S1.

Antimicrobial activity of oryzalexin S and oryzalactone

Rice blast fungi (*Pyricularia oryzae* Cavara, race 007, Naga 69-150; MAFF 101001; MAFF 101447; MAFF 101519) were obtained from

the stock culture of the Laboratory of Plant Pathology, Shimane University, and the NARO Genebank (http://www.gene.affrc.go.jp/index_en.php). *Bipolaris oryzae* (Breda de Haan) Shoemaker (MAFF 305067), *Xanthomonas oryzae* pv. *oryzae* (MAFF 210548), and *Burkholderia glumae* (MAFF 106541) were obtained from the NARO Genebank. The bioassays to evaluate antimicrobial activity were performed according to previously reported studies (Kariya et al., 2023; Murata et al., 2019).

ACKNOWLEDGEMENT

This work was supported by JSPS KAKENHI, Grant Numbers 21J23445 and 20H02923 for KK and AI, respectively.

CONFLICT OF INTEREST

The authors declare that they have no known competing financial interests or personal relationships that could have appeared to influence the work reported in this paper.

DATA AVAILABILITY STATEMENT

All data generated during this study are either included in this published article and its supplementary information files, or available from the corresponding author on request.

SUPPORTING INFORMATION

Additional Supporting Information may be found in the online version of this article.

Figure S1. Phenotype and genotype of the F_2 population generated from cv. WRC47 and cv. Kasalath.

Figure S2. Alignment of *KSLX-OL*-WRC42, WRC47, WRC68, *KSL8-jap*, and *KSL8-ind*.

Figure S3. Comparison of the full-length sequences of chromosome 11 and genomic region near *KSL9-KSL8* between cv. Nipponbare and cv. TG81.

Figure S4. Chemical structure of **1**.

Figure S5. GC–MS analysis of extracts from *Nicotiana benthamiana* leaf expressing KSLX-NOL.

Figure S6. Distribution of *KSL8*, *KSL9*, and *KSLX* in 445 accessions of *Oryza rufipogon*.

Figure S7. Phylogenetic relationship of *KSLX*s in *KSL8-KSL9-KSLX*- and in *KSLX*-possessing strains (a) and *KSL8*s in *KSL8-KSL9-KSLX*- and in *KSL8-KSL9*-possessing strains (b).

Figure S8. Phylogenetic tree of the genes homologous to the rice kaurene synthase gene (*OsKS1*).

Figure S9. Distribution of *KSL8*, *KSL9*, and *KSLX* in the genus *Oryza*.

Figure S10. Phylogenetic tree of *KSL8*, *KSL9*, and *KSLX* homologs in the AA, BB, and FF genome species in the genus *Oryza*.

Figure S11. Genetic distance of the corresponding exons and introns of *KSL8*s, *KSL9*s, and *KSLX*s.

Figure S12. Antimicrobial activity of oryzalactone and oryzalexin S.

Figure S13. Duplication timing of *mrcaKSL* affects the topology of phylogenetic tree generated by *KSL8*, *KSL9*, and *KSLX*.

Figure S14. Relative expression levels of *KSL8-jap* and *KSLX* in rice.

Figure S15. ^{1}H-NMR spectrum of **1**.

Figure S16. ^{13}C-NMR spectrum of **1**.

Figure S17. DEPT-135 of **1**.

Figure S18. ^{1}H-^{1}H COSY spectrum of **1**.

Figure S19. HMQC spectrum of **1**.

Figure S20. HMBC spectrum of **1**.

Figure S21. NOESY spectrum of **1**.

Table S1. SNPs specific to cv. WRC42, WRC47, and WRC68 and marker positions for PCR-based genotyping.

Table S2. ^{1}H- (600 MHz) and ^{13}C-NMR (150 MHz) data of **1** in $CDCl_3$.

Table S3. *KSL8*, *KSL9*, and *KSLX* genotypes of WRC cultivars and *Oryza rufipogon* strains.

Table S4. Percentages of the sequences mapped to *KSL8* and *KSLX*, and genotypes of 445 accessions of *Oryza rufipogon*.

Table S5. Primers used in this study.

Table S6. WGS data accessions.

Method S1. Supporting experimental procedures.

REFERENCES

Aggarwal, R.K., **Brar, D.S.** & **Khush, G.S.** (1997) Two new genomes in the Oryza complex identified on the basis of molecular divergence analysis using total genomic DNA hybridization. *Molecular & General Genetics*, **254**, 1–12. Available from: https://doi.org/10.1007/s004380050384

Ahuja, I., **Kissen, R.** & **Bones, M.A.** (2012) Phytoalexins in defense against pathogens. *Trends in Plant Science*, **17**(2), 73–90. Available from: https://doi.org/10.1016/j.tplants.2011.11.002

Akagi, A., **Fukushima, S.**, **Okada, K.**, **Jiang, J.C.**, **Yoshida, R.**, **Nakayama, A.** ***et al.*** (2014) WRKY45-dependent priming of diterpenoid phytoalexin biosynthesis in rice and the role of cytokinin in triggering the reaction. *Plant Molecular Biology*, **86**, 171–183. Available from: https://doi.org/10.1007/s11103-014-0221-x

Ammiraju, J.S.S., **Fan, C.**, **Yu, Y.**, **Song, X.**, **Cranston, K.A.**, **Pontaroli, A.C.** ***et al.*** (2010) Spatio-temporal patterns of genome evolution in allotetraploid species of the genus *Oryza*. *The Plant Journal*, **63**(3), 430–442. Available from: https://doi.org/10.1111/j.1365-313X.2010.04251.x

Cabanettes, F. & **Klopp, C.** (2018) D-GENIES: dot plot large genomes in an interactive, efficient and simple way. *PeerJ*, **6**, e4958. Available from: https://doi.org/10.1093/molbev/msx282

Capella-Gutiérrez, S., **Silla-Martínez, J.M.** & **Gabaldón, T.** (2009) trimAl: a tool for automated alignment trimming in large-scale phylogenetic analyses. *Bioinformatics*, **25**(15), 1972–1973. Available from: https://doi.org/10.1093/bioinformatics/btp348

Chen, F., **Tholl, D.**, **Bohlmann, J.** & **Pichersky, E.** (2011) The family of terpene synthases in plants: a mid-size family of genes for specialized metabolism that is highly diversified throughout the kingdom. *The Plant Journal*, **66**(1), 212–229. Available from: https://doi.org/10.1111/j.1365-313X.2011.04520.x

Desmedt, W., **Kudjordjie, N.E.**, **Chavan, N.S.**, **Zhang, J.**, **Li, R.**, **Yang, B.** ***et al.*** (2022) Rice diterpenoid phytoalexins are involved in defence against parasitic nematodes and shape rhizosphere nematode communities. *New Phytologist*, **235**, 1231–1245. Available from: https://doi.org/10.1111/nph.18152

Goktay, M., **Fulgione, A.** & **Hancock, A.M.** (2020) A new catalog of structure variants in 1301 *A. thaliana* lines from Africa, Eurasia, and North America reveals a signature of balancing selection at defense response genes. *Molecular Biology and Evolution*, **38**(4), 1498–1511. Available from: https://doi.org/10.1093/molbev/msaa309

Hanano, S. & **Goto, K.** (2011) *Arabidopsis* TERMINAL FLOWER1 is involved in the regulation of flowering time and inflorescence development through transcriptional repression. *The Plant Cell*, **23**, 3172–3184. Available from: https://doi.org/10.1105/tpc.111.088641

Hiei, T., **Ohta, S.**, **Komari, T.** & **Kumashiro, T.** (1994) Efficient transformation of rice (*Oryza sativa* L.) mediated by *Agrobacterium* and sequence analysis of the boundaries of the T-DNA. *The Plant Journal*, **6**(2), 271–282. Available from: https://doi.org/10.1046/j.1365-313x.1994.6020271.x

Hoang, D.T., **Chernomor, O.**, **von Haeseler, A.**, **Minh, B.Q.** & **Vinh, L.S.** (2018) UFBoot2: improving the ultrafast bootstrap approximation. *Molecular Biology and Evolution*, **35**(2), 518–522. Available from: https://doi.org/10.1093/molbev/msx281

Huang, X., **Kurata, N.**, **Wei, X.**, **Wang, Z.-X.**, **Wang, A.** ***et al.*** (2012) A map of rice genome variation reveals the origin of cultivated rice. *Nature*, **490** (7421), 497–501. Available from: https://doi.org/10.1038/nature11532

Jain, C., **Khatana, S.** & **Vijayvergia, R.** (2018) Bioactivity of secondary metabolites of various plants: a review. *International Journal of Pharmaceutical Sciences and Research*, **10**(2), 494–504. Available from: https://doi.org/10.13040/IJPSR.0975-8232.10(2).494-04

Kajiya-Kanegae, H., **Ohyanagi, H.**, **Ebata, T.**, **Tanizawa, Y.**, **Onogi, A.**, **Sawada, Y.** ***et al.*** (2021) OryzaGenome2.1: database of diverse genotypes in wild *Oryza* species. *Rice*, **14**, 24. Available from: https://doi.org/10.1093/molbev/msx284

Kariya, K., **Fujita, A.**, **Ueno, M.**, **Yoshikawa, T.**, **Teraishi, M.**, **Taniguchi, Y.** ***et al.*** (2023) Natural variation of diterpenoid phytoalexins in rice: aromatic diterpenoid phytoalexins in specific cultivars. *Phytochemistry*, **211**, 113708. Available from: https://doi.org/10.1016/j.phytochem.2023.113708

Kariya, K., **Murata, K.**, **Kokubo, Y.**, **Ube, N.**, **Ueno, K.**, **Yabuta, Y.** ***et al.*** (2019) Variation of diterpenoid phytoalexin oryzalexin A production in cultivated and wild rice. *Phytochemistry*, **166**, 112057. Available from: https://doi.org/10.1016/j.phytochem.2019.112057

Kariya, K., **Ube, N.**, **Ueno, M.**, **Teraishi, M.**, **Okumoto, Y.**, **Mori, N.** ***et al.*** (2020) Natural variation of diterpenoid phytoalexins in cultivated and wild rice species. *Phytochemistry*, **180**, 112518. Available from: https://doi.org/10.1016/j.phytochem.2020.112518

Katoh, K. & **Standley, D.M.** (2013) MAFFT multiple sequence alignment software version 7: improvements in performance and usability. *Molecular Biology and Evolution*, **30**(4), 772–780. Available from: https://doi.org/10.1093/molbev/mst010

Kawahara, Y., **de la Bastide, M.**, **Hamilton, J.P.**, **Kanamori, H.**, **McCombie, W.R.**, **Ouyang, S.** ***et al.*** (2013) Improvement of the *Oryza sativa* Nipponbare reference genome using next generation sequence and optical map data. *Rice*, **6**(1), 4. Available from: https://doi.org/10.1186/1939-8433-6-4

Kitaoka, N., **Zhang, J.**, **Oyagbenro, R.K.**, **Brown, B.**, **Wu, Y.**, **Yang, B.** ***et al.*** (2021) Interdependent evolution of biosynthetic gene clusters for momilactone production in rice. *The Plant Cell*, **33**, 290–305. Available from: https://doi.org/10.1093/plcell/koaa023

Kliebenstein, D.J., **Kroymann, J.**, **Brown, P.**, **Figuth, A.**, **Pedersen, D.**, **Gershenzon, J.** ***et al.*** (2001) Genetic control of natural variation in *Arabidopsis* glucosinolate accumulation. *Plant Physiology*, **126**(2), 811–825. Available from: https://doi.org/10.1104/pp.126.2.811

Kliebenstein, D.J., **Lambrix, V.M.**, **Reichelt, M.**, **Gershenzon, J.** & **Mitchell-Olds, T.** (2001) Gene duplication in the diversification of secondary metabolism: tandem 2-oxoglutarate-dependent dioxygenases control glucosinolate biosynthesis in *Arabidopsis*. *The Plant Cell*, **13**, 681–693. Available from: https://doi.org/10.1105/tpc.13.3.681

Koenig, D., **Hagmann, J.**, **Li, R.**, **Bemm, F.**, **Slotte, T.**, **Neuffer, B.** ***et al.*** (2019) Long-term balancing selection drives evolution of immunity genes in *Capsella*. *eLife*, **8**, e43606. Available from: https://doi.org/10.7554/eLife.43606

Kojima, Y., **Ebana, K.**, **Fukuoka, S.**, **Nagamine, T.** & **Kawase, M.** (2005) Development of an RFLP-based rice diversity research set of germplasm. *Breeding Science*, **55**(4), 431–440. Available from: https://doi.org/10.1270/jsbbs.55.431

Kroymann, J., **Donnerhacke, S.**, **Schnabelrauch, D.** & **Mlichell, O.T.** (2003) Evolutionary dynamics of an Arabidopsis insect resistance quantitative trait locus. *Proceedings of the National Academy of Sciences of the United States of America*, **100**(suppl_2), 14587–14592. Available from: https://doi.org/10.1073/pnas.1734046100

Li, D., **Liu, C.**, **Luo, R.**, **Sadakane, K.** & **Lam, T.** (2015) MEGAHIT: an ultra-fast single- 51 node solution for large and complex metagenomics assembly via succinct *de Bruijn* graph. *Bioinformatics*, **31**, 1674–1676. Available from: https://doi.org/10.1093/bioinformatics/btv033

Li, R., **Zhang, J.**, **Li, Z.**, **Peters, R.J.** & **Yang, B.** (2021) Dissecting the labdane-related diterpenoid biosynthetic gene clusters in rice reveals directional cross-cluster phytotoxicity. *New Phytologist*, **233**, 878–889. Available from: https://doi.org/10.1111/nph.17806

Lu, X., **Zhang, J.**, **Brown, B.**, **Li, R.**, **Rodriguez-Romero, J.**, **Berasategui, A.** ***et al.*** (2018) Inferring roles in defense from metabolic allocation of rice diterpenoids. *The Plant Cell*, **30**(5), 1119–1131. Available from: https://doi.org/10.1105/tpc.18.00205

Mao, L., **Kawaide, H.**, **Higuchi, T.**, **Chen, M.**, **Miyamoto, K.**, **Hirata, Y.** ***et al.*** (2020) Genomic evidence for convergent evolution of gene clusters for momilactone biosynthesis in land plants. *Proceedings of the National Academy of Sciences of the United States of America*, **117**(22), 12472–12480. Available from: https://doi.org/10.1073/pnas.1914373117

Minh, B.Q., **Schmidt, H.A.**, **Chernomor, O.**, **Schrempf, D.**, **Woodhams, M.D.**, **von Haeseler, A.** & **Lanfear, R.** (2020) IQ-TREE 2: New models and efficient methods for phylogenetic inference in the genomic era. *Molecular Biology and Evolution*, **37**(5), 1530–1534. Available from: https://doi.org/10.1093/molbev/msaa015

Miyamoto, K., **Fujita, M.**, **Shenton, M.R.**, **Akashi, S.**, **Sugawara, C.**, **Sakai, A.** ***et al.*** (2016) Evolutionary trajectory of phytoalexin biosynthetic gene clusters in rice. *The Plant Journal*, **87**, 293–304. Available from: https://doi.org/10.1111/tpj.13200

Morrone, D., **Jin, Y.H.**, **Xu, M.M.**, **Choi, S.Y.**, **Coates, R.M.** & **Peters, R.J.** (2006) An unexpected diterpene cyclase from rice: functional identification of a stemodene synthase. *Archives of Biochemistry and Biophysics*, **448**, 133–140.

Morrone, D., **Xu, M.**, **Fulton, D.B.**, **Determan, M.K.** & **Peters, R.J.** (2008) Increasing complexity of a diterpene synthase reaction with a single residue switch. *Journal of the American Chemical Society*, **130**(16), 5400–5401.

Murata, K., **Kitano, T.**, **Yoshimoto, R.**, **Takata, R.**, **Ube, N.**, **Ueno, K.** ***et al.*** (2019) Natural variation in the expression and catalytic activity of a naringenin 7-*O*-methyltransferase influences antifungal defenses in diverse rice cultivars. *The Plant Journal*, **101**, 1103–1117. Available from: https://doi.org/10.1111/tpj.14577

Nemoto, T., **Cho, E.**, **Okada, A.**, **Okada, K.**, **Otomo, K.**, **Kanno, Y.** ***et al.*** (2004) Stemar-13-ene synthase, a diterpene cyclase involved in the biosynthesis of the phytoalexin oryzalexin S in rice. *FEBS Letters*, **571**(1–3), 182–186. Available from: https://doi.org/10.1016/j.febslet.2004.07.002

Otomo, K., **Kanno, Y.**, **Motegi, A.**, **Kenmoku, H.**, **Yamane, H.**, **Mitsuhashi, W.** ***et al.*** (2004) Diterpene cyclases responsible for the biosynthesis of phytoalexins, momilactones A, B, and oryzalexins A-F in rice. *Bioscience, Biotechnology, and Biochemistry*, **68**(9), 2001–2006. Available from: https://doi.org/10.1271/bbb.68.2001

Sakamoto, T., **Miura, K.**, **Itoh, H.**, **Tatsumi, T.**, **Ueguchi-Tanaka, M.**, **Ishiyama, K.** ***et al.*** (2004) An overview of gibberellin metabolism enzyme genes and their related mutants in rice. *Plant Physiology*, **134**(4), 1642–1653. Available from: https://doi.org/10.1104/pp.103.033696

Sentoku, N., **Sato, Y.** & **Matsuoka, M.** (2000) Overexpression of rice OSH genes induces ectopic shoots on leaf sheaths of transgenic rice plants. *Developmental Biology*, **220**, 358–364. Available from: https://doi.org/10.1093/molbev/msx283

Stein, J.C., **Yu, Y.**, **Copetti, D.**, **Zwickl, D.J.**, **Zhang, L.**, **Zhang, C.** ***et al.*** (2018) Genomes of 13 domesticated and wild rice relatives highlight genetic conservation, turnover and innovation across the genus *Oryza*. *Nature Genetics*, **50**, 285–296. Available from: https://doi.org/10.1038/s41588-018-0040-0

Tanaka, N., **Shenton, M.**, **Kawahara, Y.**, **Kumagai, M.**, **Sakai, H.**, **Kanamori, H.** ***et al.*** (2020) Whole-genome sequencing of the NARO world rice core collection (WRC) as the basis for diversity and association studies. *Plant and Cell Physiology*, **61**, 922–932. Available from: https://doi.org/10.1093/pcp/pcaa019

Toyomasu, T., **Goda, C.**, **Sakai, A.**, **Miyamoto, K.**, **Shenton, M.R.**, **Tomiyama, S.** ***et al.*** (2018) Characterization of diterpene synthase genes in the wild rice species *Oryza brachyantha* provides evolutionary insight into rice phytoalexin biosynthesis. *Biochemical and Biophysical Research Communications*, **503**, 1221–1227. Available from: https://doi.org/10.1016/j.bbrc.2018.07.028

Toyomasu, T., **Miyamoto, K.**, **Shenton, M.R.**, **Sakai, A.**, **Sugawara, C.**, **Horie, K.** ***et al.*** (2016) Characterization and evolutionary analysis of ent-kaurene synthase like genes from the wild rice species *Oryza rufipogon*. *Biochemical and Biophysical Research Communications*, **480**, 402–408. Available from: https://doi.org/10.1016/j.bbrc.2016.10.062

Toyomasu, T., **Shenton, M.R.** & **Okadam, K.** (2020) Evolution of labdane-related diterpene synthases in cereals. *Plant and Cell Physiology*, **61**(11), 1850–1859. Available from: https://doi.org/10.1093/pcp/pcaa106

Valletta, A., **Iozia, L.M.**, **Fattorini, L.** & **Leonelli, F.** (2023) Rice phytoalexins: half a century amazing discoveries; part I: distribution, biosynthesis, chemical synthesis, and biological activities. *Plants*, **12**, 260. Available from: https://doi.org/10.3390/plants12020260

Vasimuddin, M., **Misra, S.**, **Li, H.** & **Aluru, S.** (2019) Efficient architecture-aware acceleration of BWA-MEM for multicore systems. In: *IEEE Parallel*

and Distributed Processing Symposium. Rio de Janeiro: IEEE, pp. 314–324. Available from: https://doi.org/10.1109/IPDPS.2019.00041

Wang, S., **Alseekh, S.**, **Fernie, A.R.** & **Luo, J.** (2019) The structure and function of major plant metabolite modifications. *Molecular Plant*, **12**(7), 899–919. Available from: https://doi.org/10.1016/j.molp.2019.06.001

Wu, D., **Hu, Y.**, **Akashi, S.**, **Nojiri, H.**, **Guo, L.**, **Ye, C.** ***et al.*** (2022) Lateral transfers lead to the birth of momilactone biosynthetic gene clusters in grass. *The Plant Journal*, **111**(5), 1354–1367.

Xu, M., **Wilderman, P.R.** & **Peters, R.J.** (2007) Following evolution's lead to a single residue switch for diterpene synthase product outcome. *Proceedings of the National Academy of Sciences of the United States of America*, **104**(18), 7397–7401. Available from: https://doi.org/10.1073/pnas.0611454104

Xu, M., **Wilderman, R.P.**, **Morrone, D.**, **Xu, J.**, **Roy, A.**, **Margis-Pinheiro, M.** ***et al.*** (2007) Functional characterization of the rice kaurene synthase-like gene family. *Phytochemistry*, **68**(3), 312–326. Available from: https://doi.org/10.1016/j.phytochem.2006.10.016

Xu, M.M., **Hillwig, M.L.**, **Prisic, S.**, **Coates, R.M.** & **Peters, R.J.** (2004) Functional identification of rice *syn*-copalyl diphosphate synthase and its role in initiating biosynthesis of diterpenoid phytoalexin/allelopathic natural products. *The Plant Journal*, **39**, 309–318.

Yan, N., **Yang, T.**, **Yu, X.**, **Shang, L.**, **Guo, D.**, **Zhang, Y.** ***et al.*** (2022) Chromosome-level genome assembly of *Zizania latifolia* provides insights into its seed shattering and phytocassane biosynthesis. *Communications Biology*, **5**, 36. Available from: https://doi.org/10.1038/s42003-021-02993-3

Yoshida, Y., **Nosaka-T, M.**, **Yoshikawa, T.** & **Sato, Y.** (2022) Measurements of antibacterial activity of seed crude extracts in cultivated rice and wild Oryza species. *Rice*, **15**, 63. Available from: https://doi.org/10.1186/s12284-022-00610-3

Zhan, C., **Lei, L.**, **Liu, Z.**, **Zhou, S.**, **Yang, C.**, **Zhu, X.** ***et al.*** (2020) Selection of a subspecies-specific diterpene gene cluster implicated in rice disease resistance. *Nature Plants*, **6**, 1447–1454. Available from: https://doi.org/10.1038/s41477-020-00816-7

Zhang, F., **Xue, H.**, **Dong, X.**, **Li, M.**, **Zheng, X.**, **Li, Z.** ***et al.*** (2022) Long-read sequencing of 111 rice genomes reveals significantly larger pan-genomes. *Genome Research*, **32**(5), 853–863. Available from: https://doi.org/10.1101/gr.276015.121

Zhao, L., **Oyagbenro, R.**, **Feng, Y.**, **Xu, M.** & **Peters, R.J.** (2023) Oryzalexin S biosynthesis: a cross-stitched disappearing pathway. *aBIOTECH*, **4**, 1–7. Available from: https://doi.org/10.1007/s42994-022-00092-3

Zhou, Y., **Zhang, C.**, **Zhang, L.**, **Ye, Q.**, **Liu, N.**, **Wang, M.** ***et al.*** (2022) Genes fusion as an important mechanism to generate new genes in the genus *Oryza*. *Genome Biology*, **23**, 130. Available from: https://doi.org/10.1186/s13059-022-02696-w

Zust, T., **Heichinger, C.**, **Grossniklaus, U.**, **Harrington, R.**, **Kliebenstein, J.D.** & **Turnbull, A.L.** (2012) Natural enemies drive geographic variation in plant defenses. *Science*, **338**, 116–119. Available from: https://doi.org/10.1126/science.1226397